Cooperative Double Deprotonation of Bis(2-picolyl)amine Leading to Unexpected Bimetallic Mixed Valence (M^{-I}, M^{I}) Rhodium and Iridium Complexes

Cristina Tejel,[a] M. Pilar del Río,[a] Laura Asensio,[a] Fieke J. van den Bruele,[a] Miguel A. Ciriano,[a] Nearchos Tsichlis i Spithas,[b] Dennis G. H. Hetterscheid,[b] and Bas de Bruin*[b]*

[a] Instituto de Síntesis Química y Catálisis Homogénea (ISQCH), CSIC - Universidad de Zaragoza, Departamento de Química Inorgánica, Pedro Cerbuna 12, 50009-Zaragoza (Spain), Fax: (+) 34 976 761187. E-mail: ctejel@unizar.es

[b] Van 't Hoff Institute for Molecular Sciences, University of Amsterdam, Science Park 904, 1098 XH, Amsterdam (the Netherlands), Fax: (+31) 20 5255604. E-mail: b.debruin@uva.nl

Abstract: Cooperative reductive double deprotonation of the complex $[Rh^{I}(bpa)(cod)]^{+}$ ($[\mathbf{4}]^{+}$, bpa = $PyCH_2NHCH_2Py$) with one molar equivalent of base produces the bimetallic species [(cod)Rh(bpa–2H)Rh(cod)] (**7**), which displays a large Rh^{-I},Rh^{I} contribution to its electronic structure. The doubly deprotonated ligand in **7** hosts the two 'Rh(cod)' fragments in two distinct compartments: a 'square planar compartment' consisting of one of the Py donors and the central nitrogen donor, and a 'tetrahedral π-imine compartment' consisting of the other pyridine and an 'imine C=N' donor. The formation of an 'imine donor' in this process is the result of substantial electron transfer from the $\{bpa–2H\}^{2-}$ ligand to one of the rhodium centers to form the neutral imine ligand bpi (bpi = $PyCH_2N=CHPy$). Hence deprotonation of $[Rh^{I}(bpa)(cod)]^{+}$ represents a reductive process, effectively

leading to a reduction of the metal oxidation state from Rh^{I} to Rh^{-I}. The dinuclear iridium counterpart, complex **8**, can also be prepared, but it is unstable in the presence of 1 molar equivalent of the free bpa ligand leading to quantitative formation of the neutral amido mononuclear compound [Ir^{I}(bpa–H)(cod)] (**2**). All attempts to prepare the rhodium analog of **2** failed and led to spontaneous formation of **7**. The thermodynamic differences are readily explained by a lower stability of the M^{-I} oxidation state for iridium as compared to rhodium. The observed reductive double deprotonation leads to the formation of unusual structures and unexpected reactivity, which underlines the general importance of 'redox non-innocent ligands' and their substantial effect on the electronic structure of transition metals.

Introduction

Amido ligands (R_2N^-) are an interesting class of cooperating ligands allowing activation of substrates coordinated to transition metals. Cooperative substrate activation by ruthenium-amido complexes in Noyori hydrogenations provides a seminal example.[1] Rhodium-amido complexes have received considerably less attention in this field.[2] Nonetheless, some recent examples reveal that amido complexes of the type [Rh($Ntrop_2$)(PR_3)] ($Ntrop_2$ = bis(tropylidenyl)amide, R = Ph) show interesting properties, such as cooperative substrate activation in dehydrogenative coupling reactions of alcohols.[3] Closely related cooperative reduction of dioxygen can be effectively catalyzed by dinuclear amido-rhodium complexes.[4] Additionally, these types of systems are able to promote interesting reactions such as amido transfer to alkenes and vinylarenes,[5] cycloaddition reactions associated with C–N bond formation,[6] and C–Cl[7] and C–H[8] bond activation reactions. In other instances, related dinuclear complexes[9] have been used as precursors for low-valent late transition metal imido-clusters.[10] Our understanding of the redox-properties of the 'Rh–NR_2' framework is however still in its infancy, and therefore the outcome of electron transfer reactions is quite unpredictable. Nonetheless, a rich chemistry can be envisaged from both metal-centred[11] and ligand-centred oxidations.[12,13] This revealed among others the 'redox non-innocence' of the amido ligand, and the resulting aminyl radical ligands show interesting bond activations by radical hydrogen abstraction.[14]

We have previously investigated in detail the effect of one-electron oxidation of ethylene[15] and 1,5-cyclooctadiene[16] (cod) iridium complexes, and some of these investigations clearly revealed the 'redox non-innocence' of the bis(2-picolyl)amine (bpa) ligand. Furthermore, bpa deprotonation proved to have a profound effect on the properties and reactivity of $[Ir(bpa)(cod)]^+$.[17] Sequential deprotonation of $[Ir(bpa)(cod)]^+$ ($[\mathbf{1}]^+$) at the central amine donor, and subsequently the adjacent methylene moiety, allows the isolation of the neutral amido complex [Ir(bpa–H)(cod)] (**2**) and the 'de-aromatized' anionic complex $[Ir(bpa–2H)(cod)]^-$ ($[\mathbf{3}]^-$), respectively (see Scheme 1).[18] Related Ru, Rh and Ir systems have been reported by Schneider[19] and Milstein,[20] some of which are excellent catalysts for transfer hydrogenation and dehydrogenative coupling reactions and offer interesting opportunities for water splitting.

Scheme 1. Formation of neutral **2** and anionic $[\mathbf{3}]^-$ iridium complexes upon sequential deprotonation of cationic $[\mathbf{1}]^+$ and the double deprotonation of the rhodium complex $[\mathbf{4}]^+$ to $[\mathbf{6}]^-$.

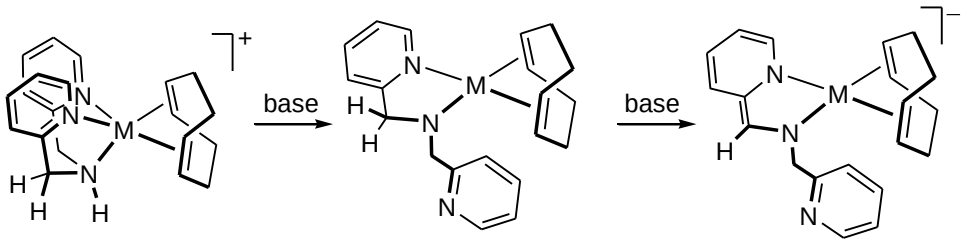

Inspired by the deprotonation results of the iridium complexes, and motivated by the interesting literature precedents concerning amido ligand cooperativity in rhodium-mediated hydrogenation catalysis and the redox non-innocence of rhodium-amido complexes revealing intriguing atom abstraction reactions, we decided to investigate the deprotonation of the cationic $[Rh(bpa)(cod)]^+$ complex.[21] We aimed at preparing the neutral rhodium amido complex [Rh(bpa–H)(cod)] (**5** in Scheme 1) to investigate its reactivity. However, quite unexpectedly, it turned out that a *cooperative reductive*

double deprotonation process rendering a mixed-valence dinuclear complex takes place. The reason behind this unusual behaviour and the unexpected results are the topics of this paper.

Results and Discussion

Cooperative double deprotonation of [Rh(bpa)(cod)]$^+$. In an initial attempt to prepare the neutral rhodium-amido complex [Rh(bpa–H)(cod)], the compound [Rh(bpa)(cod)]PF_6 ([**4**]PF_6) was treated with 1 molar equivalent of KO^{t}Bu in thf at room temperature. This did *not* produce the expected neutral square planar rhodium complex (**5**, Scheme 1). Only 1 equivalent of the base was enough to achieve the full conversion of [**4**]$^+$ into the asymmetric dinuclear complex [(cod)Rh(bpa–2H)Rh(cod)] (**7**) along with free bpa in a 1:1 molar ratio (Scheme 2).

Scheme 2. Cooperative double deprotonation of [**4**]$^+$ leading to formation of the dinuclear complex [(cod)Rh(bpa–2H)Rh(cod)] (**7**) and free bpa.

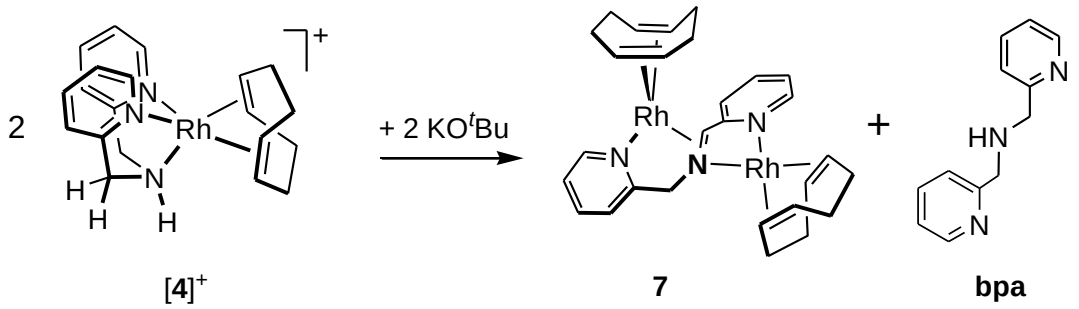

In several other experiments, using ≤ 1 equivalent of the base, we always obtained the same result. Treatment of [**4**]$^+$ with ≥ 2 equivalents of the base, however, produced readily and in a quantitative way the doubly deprotonated compound K[Rh(bpa–2H)(cod)] (K[**6**], Scheme 1), which contains a 'de-aromatized' pyridine moiety.[18a] Moreover, addition of [**4**]$^+$ to thf-d_8 solutions of K[**6**] at room temperature did not produce the expected acid/base comproportionation of the ligand to [Rh(bpa–H)(cod)] (as the iridium counterpart does). On the contrary, complex **7** and free bpa were the

sole products from the reaction (Scheme 3). Furthermore, monitoring the reaction of $[\mathbf{4}]^+$ and KO^{t}Bu (1:1 molar ratio) at −70º C in thf-d_8 allowed the observation of $[\mathbf{6}]^-$ in the reaction medium (along with the starting $[\mathbf{4}]^+$ and small amounts of the products: **7** and free bpa). No evidence for [Rh(bpa–H)(cod)] was found in any experiment.

Scheme 3. Typical acid/base behavior for iridium and cooperative reductive double deprotonation for rhodium.

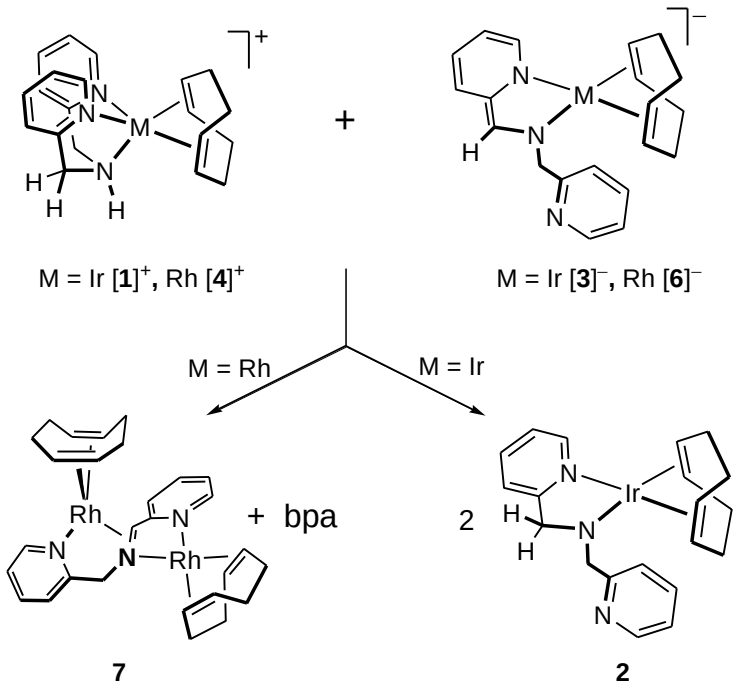

It thus seems that deprotonation with only one equivalent of base leads to a cooperative double deprotonation to the anionic $[Rh(bpa–2H)(cod)]^-$ ($[\mathbf{6}]^-$), which abstracts a 'Rh(cod)' moiety from the remaining cationic complex $[Rh(bpa)(cod)]^+$ ($[\mathbf{4}]^+$) complexes to give **7** along with liberation of an equivalent of the free bpa ligand. This is a thermodynamically driven reaction (*vide infra*).

Sequential acid deprotonation and base protonation generally becomes increasingly difficult after each step as a result of charge accumulation ($K_{a1} > K_{a2}$), and the reverse behaviour ($K_{a1} < K_{a2}$) associated with cooperative (de)protonation is rare. Some examples of increased amine basicity of macrocyclic proton receptors after the first protonation have been explained by conformational rearrangements

enforcing hydrogen bonding and/or by the encapsulation of mediating water molecules.[22] Apart from these clear examples, a few less-defined examples of (mononuclear) metal-ion induced cooperative deprotonation and coordination of peptide-based ligands in water have been reported, but the cooperativity was not explained.[23] Chelation (i.e. bringing the fragments closer to the metal) and solvation must have played an important role in these observations.[24] We are not aware of any examples of cooperative deprotonation sequences of coordinated ligands (mononuclear complexes).

In a similar way, reaction of [{Rh(cod)(μ-OMe)}$_2$] with bpa (in 1:2 molar ratio) again produces the neutral [(cod)Rh(bpa–2H)Rh(cod)] (**7**) and free bpa without evidence of mononuclear [Rh(bpa–H)(cod)]. According to the stoichiometry of the reaction, complex **7** was cleanly prepared by reacting [{Rh(cod)(μ-OMe)}$_2$] and bpa (1:1 molar ratio) in diethyl ether. From these solutions complex **7** was isolated as dark red microcrystals suitable for X-ray diffraction studies.

Molecular structure of [(cod)Rh(bpa–2H)Rh(cod)] (7). The molecular structure of **7** is shown in Figure 1 along with the labelling scheme used. Selected bond distances and angles are collected in Table 1.

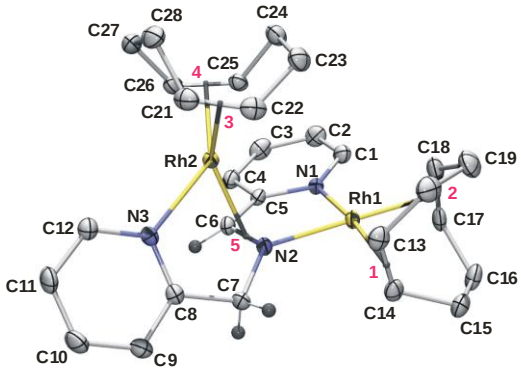

Figure 1. Molecular structure (ORTEP at 50% level) of complex **7**. Numbers in purple corresponds to the middle points (centroids) of the coordinated double bonds.

Table 1. Selected bond distances (Å) and angles (º) for complexes [(cod)M^{-I}(bpa–2H)M^{I}(cod)] (M = Rh, **7**; Ir, **8**).

	7	**8**		**7**	**8**
M1–N1	2.094(2)	2.081(5)	M2–N3	2.216(2)	2.166(5)
M1–N2	2.032(2)	2.028(5)	M2–Ct5[a]	2.076(3)	2.078(6)
M1–Ct1[a]	2.010(3)	2.005(6)	M2–Ct3[a]	2.043(3)	2.036(7)
M1–Ct2[a]	1.997(3)	1.981(6)	M2–Ct4[a]	1.964(3)	1.953(6)
M2-N2	2.254(2)	2.247(5)	M2-C6	2.130(3)	2.145(6)
C13–C14	1.394(4)	1.408(9)	C21–C22	1.396(4)	1.401(9)
C17–C18	1.401(4)	1.418(9)	C25–C26	1.427(4)	1.458(8)
N1–C1	1.355(4)	1.366(7)	C1–C2	1.369(4)	1.360(8)
C2–C3	1.401(5)	1.399(9)	C3–C4	1.374(4)	1.371(9)
C4–C5	1.407(4)	1.395(8)	C5–N1	1.373(4)	1.374(7)
C5–C6	1.434(4)	1.440(8)	C6–N2	1.415(4)	1.427(7)
N2–C7	1.460(4)	1.467(7)	C7–C8	1.509(4)	1.495(8)
C8–N3	1.341(4)	1.346(7)	C8–C9	1.400(4)	1.391(8)
C9–C10	1.374(4)	1.376(9)	C10–C11	1.388(5)	1.401(9)
C11–C12	1.375(4)	1.378(8)	C12–N3	1.354(4)	1.356(8)
N1–M1–Ct1	173.6(1)	173.1(2)	N3–M2–Ct3	98.7(1)	98.0(2)
N2–M2–Ct2	175.7(1)	174.9(2)	Ct4–M2–Ct5	120.1(1)	118.1(2)
N1–M1–N2	80.4(1)	79.8(2)	N3–M2–Ct5	78.2(1)	78.4(2)
Ct1–M1–Ct2	87.7(1)	87.0(2)	Ct3–M2–Ct4	87.1(1)	86.8(2)

[a] Ct1, Ct2, Ct3, Ct4 and Ct5 are the middle points between C13 and C14, C17 and C18, C21 and C22, C25 and C26, and C6 and N2, respectively.

The {bpa–2H} ligand in **7** acts as a hetero-dicompartmental ligand, hosting the two 'Rh(cod)' fragments in two distinct compartments. The first compartment functions as a heterobidentate N,N'-ligand consisting of one of the Py donors and the central amido nitrogen (N2), thus hosting a Rh(cod) fragment (Rh1). The coordination geometry around Rh1 is clearly square planar, with only a small twist (5.7(2)º) of the planes defined by N1–Rh1–N2 and Ct1–Rh1–Ct2 (Figure 1). The other Py-donor and the C6–N2 π bond are coordinated to the second Rh atom. The angles around N2 (if Rh2 is not

considered) are close to 120º, and their sum (Σ^0 = 356º) is close to the expected value for an sp^2 hybridized nitrogen (Rh1–N2–C7 126.7(2)º, Rh1–N2–C6 113.7(2)º, and C6–N2–C7 115.2(2)º). A similar geometry is observed for C6 with values of 117.7(19), 116.1(19) and 116.0(2)º for the angles N2–C6–H6, C5–C6–H6, and C5–C6–N2, respectively, although their sum (Σ^0 = 350º) suggests same pyramidalization consequence of the π-coordination of Rh2. In addition, the maximum deviation from the best plane defined by the five-membered rhodacycle Rh1–N1–C5–C6–N2 is only 0.092 Å. Therefore, N2 and C6 can be described as sp^2-hybridized atoms, pointing to a relatively strong imine character of the C6–N2 bond. In fact, a relatively short C6–N2 bond length (1.415(4) Å) is observed. Although the C=N bond distance in aromatic free imines lies in the range 1.25-1.33 Å, this distance should be enlarged by the π-coordination to rhodium.

In this perspective, the 'imine' is π-coordinated to Rh2, and as such, the geometry around this 'four-coordinate' Rh2 centre is perhaps best described as distorted tetrahedral. The dihedral angle between the Ct5-Rh2-N3 and Ct3-Rh2-Ct4 planes (56.5(2)º) lies intermediate between tetrahedral (90º) and square planar (0º), although clearly greatly distorted from the latter (Figure 1). These structural data suggest that the bpa–2H bridging ligand in **7** is, in fact largely transformed into the imine PyCH=N–CH_2Py (bpi) ligand by transfer of almost two electrons from the initially dianionic $\{bpa–2H\}^{2–}$ ligand to rhodium with concomitant reduction of this rhodium centre to $Rh^{–I}$. Accordingly, the Rh2–N distances (Rh2–N2: 2.254(2) Å, Rh2–N3: 2.216(2) Å) are longer than the Rh1–N distances (Rh1–N1; 2.094(2) and Rh1–N2: 2.032(2) Å) as expected for a reduced rhodium(–I) center. In good agreement, Rh2 seems to adopt an almost tetrahedral geometry, typical for d^{10}-ML_4 complexes. All these features are similar to the complex [(nbd)Rh(bpa–2H)Rh(ndb)] previously communicated.[25]

The structural data suggest that resonance structure $\mathbf{7^A}$ (Scheme 4) contributes substantially to the electronic structure of **7**.[26] Nevertheless, a second resonance structure with a Rh^I ion being part of a rhoda(I)-aza-cyclopropane ring ($\mathbf{7^B}$, Scheme 4), cannot be completely neglected

Scheme 4. Contributing resonance structures of complex **7**.

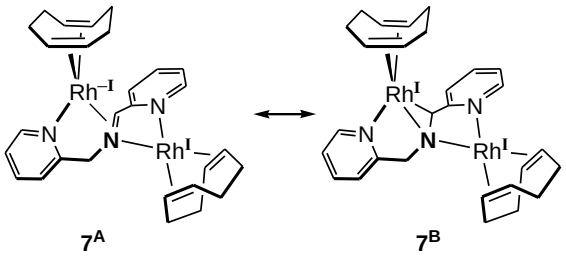

7A **7B**

For the main resonance form (**7A**) the square-planar Rh^{I} can be considered as a d^8 cationic 16 VE (VE = valence electron) centre to which the bpi ligand contributes with four electrons. The tetrahedral Rh^{-I} is a d^{10} anionic 18 VE centre to which the bpi also contributes with four electrons. Consequently, complex **7** can be considered, in part, as a zwiterionic complex. Resonance structure **7B** leads to an identical electron count for both rhodium atoms, in which case the bridging $\{bpa\text{-}2H\}^{2-}$ ligand is a 10e donor ligand (4e to Rh1 and 6e to Rh2).

DFT modelling of [(cod)Rh(bpa−2H)Rh(cod)] (7). The DFT-optimized geometry of **7** (Figure 2) is very close to the X-ray structure (Figure 1). The species is clearly diamagnetic. A closed-shell ground state is expected for second row metals, but nonetheless we checked for a possible singlet biradical ground state with two antiferromagnetically coupled electrons with broken-symmetry U–DFT calculations. These, however, in all possible attempts, converged to the same closed-shell singlet configuration as in the restricted closed-shell DFT calculations. Metal-ligand biradical descriptions can thus be excluded. The DFT calculations indicate strong Rh d-orbital mixing, which complicates a direct and simple interpretation of its electronic structure. A Löwdin orbital occupancy analysis (b3-lyp, TZVP) indicates that both Rh atoms in **7** have a total d-orbital occupancy of almost exactly 8 electrons (Rh1: 8.0e; Rh2: 8.1e). These values does not allow us to unambiguously discriminate between the resonance structures in Scheme 4, since for the Rh^{I} based resonance structure **7B** and for the Rh^{-I} based resonance structure **7A**, with substantial π-back donation to the 'imine' ligand π*-orbitals, one expects to find such values. It thus seems that the Rh^{-I}-imine π-bond is associated with a strong covalency, and

hence the electronic structure of **7** is best described being somewhere in between the resonance structures $\mathbf{7^A}$ and $\mathbf{7^B}$, with a rather large relative contribution of $\mathbf{7^A}$.

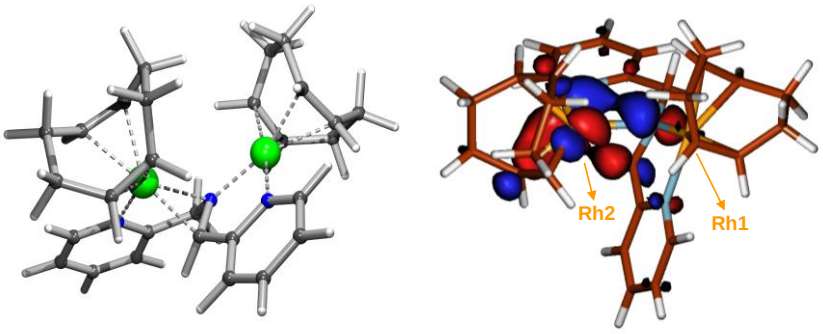

Figure 2. DFT optimized geometry (left) and HOMO (right) of **7**.

It should be indicated that late transition metal complexes with a η^2-C=N bonded moiety are very scarce and that they are systematically described as metalla-aza-cyclopropanes ($\mathbf{7^B}$, Scheme 4) in complexes of palladium[27] and iridium.[28] The single related precedent in rhodium chemistry corresponds to the complex [Rh(CH_2Ntrop$_2$)(PR_3)] (HNtrop$_2$ = bis(tropylidenyl)amine, R = Ph) described by Grützmacher,[29] of which the structural parameters point to a rhoda-aza-cyclopropane rather than a η^2-iminium ion bound to a reduced metal. In addition, related two-electron mixed-valence complexes M(0,II)[30] have been synthesized using special ligands capable of stabilizing redox asymmetric environments as developed by Nocera et al.[31] Some of them show interesting new mechanisms in hydrogenation reactions,[32] C–H activation reactions,[33] and are photoactive in hydrogen production.[34] Very recently, an unusual Rh(–I,III) complex has been reported.[35]

NMR spectra of [(cod)Rh(bpa–2H)Rh(cod)] (7). The unusual structure of **7** is maintained in solution according to multinuclear NMR spectra. Figure 3 shows the ^{1}H NMR spectrum of **7** in C_6D_6, while a selected region of the $^{13}C\{^1H\}$ NMR spectrum is included in the inset. The methylene protons from the intact CH_2 group give rise to an AB spin system centred at δ 4.18 ppm, while the proton from the imine (HC=N) produces a singlet at δ 4.32 ppm.

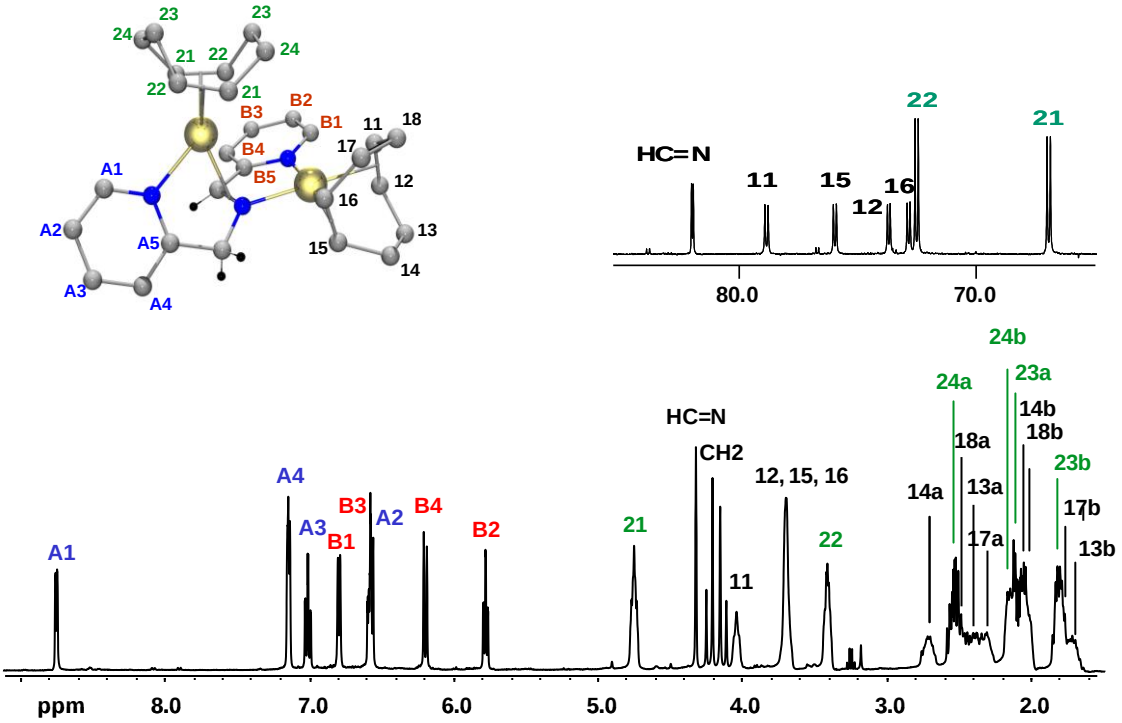

Figure 3. ^{1}H NMR spectrum in C_6D_6 of **7**. A selected region of the $^{13}C\{^{1}H\}$-apt NMR spectrum in shown in the inset.

The quite different nature of the corresponding carbon atoms is detected in the $^{13}C\{^{1}H\}$ NMR spectrum, where the CH_2 group resonates at the usual chemical shift (δ 60.53 ppm, $J_{C,Rh}$ = 1.5 Hz), while the signal for the HC=N carbon is shifted to low-field (δ 82.23 ppm, $J_{C,Rh}$ = 7.6 Hz). The two inequivalent pyridine rings give rise to two well-defined sets of four signals each one, easily identified from the ^{1}H,^{1}H-cosy and ^{1}H,^{1}H-noesy spectra. Thus, the two cross-peaks due to nOe effect between the CH_2 and A^4 protons and between the HC=N and B^4, respectively, unequivocally correspond to the connectivity shown in Figure 3. The signals of the nearby pyridine moiety of **7** (labelled in red) are substantially upfield shifted (up to δ 5.8 ppm) suggesting some delocalization of electronic density of the bridging ligand into this pyridine ring.

The cod ligands also behave in a distinct way; one of them [cod(2)] appears to have an averaged C_2 symmetry on the NMR time scale, thus producing two olefinic resonances in the ^{1}H NMR spectrum and two in the $^{13}C\{^{1}H\}$-apt spectrum (see inset in Figure 3). The other, [cod(1)], is observed as a typical cod

ligand lacking elements of symmetry. The olefinic protons H^{21} and H^{22} of the fluxional cod(2) give two relevant nOe cross-peaks with the pyridine A^1 and B^4 protons. Therefore, cod(2) is coordinated to the 'tetrahedral' Rh2 atom. Accordingly, the olefinic protons of the unsymmetrical cod(1) ligand give rise to the corresponding nOe cross-peaks with the B^1 proton, and with A^4 with smaller intensity, so that cod(1) is coordinated to the square-planar Rh1 atom.

The fluxional behavior undergone by cod(2) requires some comments. Apparently, the exchange can be described as the rotation of this cod ligand around the rhodium atom. Moreover, the observation of this fluxional process, which cannot be frozen even on cooling to –80 ºC in toluene-d_8, indicates that it possesses a low energy barrier. The fast rotation of cod(2) around the Rh2 center is in good agreement with the 'tetrahedral' geometry of this metal. For most square-planar d^8 Rh^I complexes this is a much higher-energy process.[36] In the Rh^{-I}(π-imine) description **7**$^{\mathbf{B}}$ (Scheme 4), the d^{10} configuration of the 'tetrahedral' Rh2 leads to a ligand field stabilization energy of zero (LFSE = 0), which may further contribute to the easy rotation of cod(2).

Synthesis of [(cod)Rh^{-I}(bpa–2H)Rh^{I}(cod)] (7) from [(cod)Rh^{I}(bpa–H)Rh^{I}(cod)]$^+$.

The two-electron mixed-valence dinuclear complex [(cod)Rh(bpa–2H)Rh(cod)] (**7**) differs in only a proton from the cationic [(cod)Rh(bpa–H)Rh(cod)]$^+$ which contains two Rh^I centers.[37] Therefore, we decided to investigate the relationships between these compounds. Indeed, addition of one mol of base to [(cod)Rh(bpa–H)Rh(cod)]$^+$ gives **7** cleanly and quantitatively. The abstraction of a proton from cationic [(cod)Rh(bpa–H)Rh(cod)]$^+$ is thus accomplished with a strong electronic reorganization, best described as a reduction of Rh^I to Rh^{-I} with oxidation of the dianionic $\{bpa–2H\}^{2–}$ ligand to a neutral imine ligand $PyCH_2N{=}CHPy$. To our best knowledge, this ligand-to-metal electron transfer upon deprotonation of [(cod)Rh(bpa–H)Rh(cod)]$^+$ to produce the redox asymmetric dinuclear rhodium complex **7** is an unprecedented reaction.[38] Moreover, under specific conditions the dinuclear cationic complex evolves to **7** even in the absence of an external base (see Scheme 5). While orange solutions of

[(cod)Rh(bpa–H)Rh(cod)]PF_6 in acetone-d_6 show a sharp ^{1}H NMR spectrum, addition of one molar-equivalent of [PPN]Cl as a chloride donor ([PNN]Cl = bis(triphenylphosphine)iminium chloride) leads to a color change of the solution from orange to red. The ^{1}H NMR signals of this mixture are substantially broadened. Chloride coordination to the organometallic cation must be the origin of the enhanced fluxionality. The disappearance of the AB pattern signals of the methylenic protons clearly reveals the cleavage of the amido-bridge, and points to the involvement of the neutral species **A** (Scheme 5). Addition of toluene-d_8 to the same NMR tube leads to a further color change to dark-red. At this point, lowering the polarity of the reaction medium by faster evaporation of acetone than toluene produces spectra showing *only* complex **7**, while a yellow solid precipitates. The yellow compound was isolated and further characterized as the complex double salt $[Rh(bpa)(cod)]^+[RhCl_2(cod)]^-$ ([**1**][$RhCl_2$(cod)]) (Scheme 5).

Scheme 5. Spontaneous proton transfer induced by chloride coordination producing **7**.

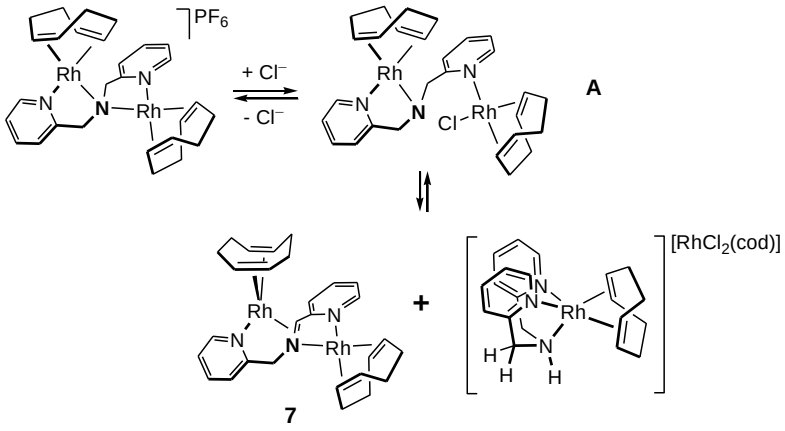

Species **A** is, in fact, a derivative of the *hypothetical* amido compound [Rh(bpa–H)(cod)] with a 'RhCl(cod)' fragment coordinated to the pendant pyridyl ring. Consequently, it undergoes the same atypical acid/base behaviour giving the {bpa–2H} ligand contained in **7** and bpa coordinated in the cation/anion complex double salt. This result represents a second example for the intrinsic instability of the 'Rh(bpa–H)(cod)' framework and its tendency towards acid/base disproportionation.

Synthesis of homodinuclear Ir^{-I},Ir^{I} and heterodinuclear Rh^{-I},Ir^{I} complexes. Considering that [Rh(bpa–2H)(cod)]$^-$ ([**6**]$^-$) is a likely intermediate in the reaction giving [(cod)Rh(bpa–2H)Rh(cod)] (**7**), we thought that the iridium counterpart [Ir(bpa–2H)(cod)]$^-$ ([**3**]$^-$) could be a useful precursor for the generation of Ir analogs of this new class of two-electron mixed-valence complexes. Consistent with these ideas, complex [Ir(bpa–2H)(cod)]$^-$ ([**3**]$^-$) reacts with [{Ir(μ-Cl)(cod)}$_2$] to give the dinuclear neutral complex [(cod)Ir(bpa–2H)Ir(cod)] (**8**). A similar reaction of anionic [**3**]$^-$ with [{Rh(μ-Cl)(cod)}$_2$] produces the heterometallic [(cod)Rh(bpa–2H)Ir(cod)] (**9**). Both complexes were isolated as air-sensitive red-brown solids. Nonetheless, the homobimetallic complex **8** is more easily obtained, in a pure form and in good yields, by reacting [{Ir(cod)(μ-OMe)}$_2$] with bpa in 1:1 molar ratio in diethyl ether, while reaction of the isolated iridium-amido complex **2** with [{Rh(cod)(μ-OMe)}$_2$] in a 2:1 molar ratio produces the hetero-dinuclear Rh,Ir complex **9** in a more selective manner. Detailed NMR spectroscopic information for these complexes is given in the Experimental Section. The X-ray geometry and the bond lengths of **7** and **8** are very similar (Table 1).

For the Rh,Ir compound **9**, ^{13}C-^{103}Rh couplings in combination with ^{1}H-^{1}H noesy experiments unequivocally establish that the 'Rh(cod)' fragment is coordinated in the 'tetrahedral π-imine compartment', while the Ir(cod) fragment is coordinated in the 'square planar compartment'. The NMR data of **9** are clean and clearly confirm the proposed structure. However, complex **9** reveals quite unusual chemical shifts of the 'imine' (and some of the pyridine signals) in the NMR spectra as compared to those of **7** and **8**. The ^{13}C signal of the bridging C=N moiety shifts, upfield from δ = 82 ppm in the Rh,Rh compound **7** to 72 ppm in the Ir,Ir compound **8**, thus reflecting the stronger covalency of the Ir–N bond. For the Rh,Ir compound **9** one would expect an intermediate chemical shift; however, it is actually observed downfield relative to **7** (δ = 93 ppm). This behaviour seems to be temperature dependent, but presently we do not entirely understand it. It seems that compound **9** is involved in a fluxional behaviour, which we are currently investigating.

Electronic structures and thermodynamic stability of amido complexes [M(bpa–H)(cod)] (M = Rh, Ir). Since the dinuclear compounds **7-9** are all isolable and stable compounds, we still wondered why the rhodium amido complex [Rh(bpa–H)(cod)] (**5**) spontaneously disproportionates to free bpa and the dinuclear complex [(cod)Rh(bpa–2H)Rh(cod)] (**7**). Are the species **2** and **5** both intrinsically unstable with respect to disproportionation to **8**/**7** and free bpa with a kinetic barrier preventing this reaction to occur for the iridium species? Or is formation of rhodium species **7** from **5** thermodynamically favoured while formation of **8** from **2** is unfavourable? We tried to answer these questions through a set of additional experiments and DFT calculations.

We first calculated the properties of the elusive compound [Rh(bpa–H)(cod)] (**5**) with DFT, in order to compare its structure and its frontier orbitals with those of the iridium analogue **2**. These calculations do not reveal any unusual geometrical differences between **2** and **5**, which are almost completely isostructural, and also the frontier orbitals of these species are nearly identical. Since the filled p-type amido lone pair of the ligand must interact with the filled metal d_π-orbitals of the d^8-transition metals, this unfavourable interaction could be considered as a π-conflict,[19a,39] which could in principle destabilize rhodium complex **5** stronger than iridium complex **2**. However, for both species this repulsive interaction is counterbalanced by an increased π-back-donation from the metal into the π* orbital of the cod double bond *trans* to the amido fragment, thus resulting in some bonding character of the resulting HOMO. The overall effect is then a net π-bonding between rhodium or iridium and the amido fragment (Figure 4).

Back-donation is generally stronger for iridium than for rhodium, which might in part explain the increased stability of iridium complex **2** compared with that of rhodium complex **5**. This is confirmed by the large upfield shifts of the olefinic carbons *trans* to the amido fragment in **2**. The DFT calculations show that the dominating differences between **2** and **5** are mainly reflecting the stronger σ-interactions of the M–N bonds in **2** (Ir) compared to **5** (Rh), which could contribute to the relative stability of **2**.

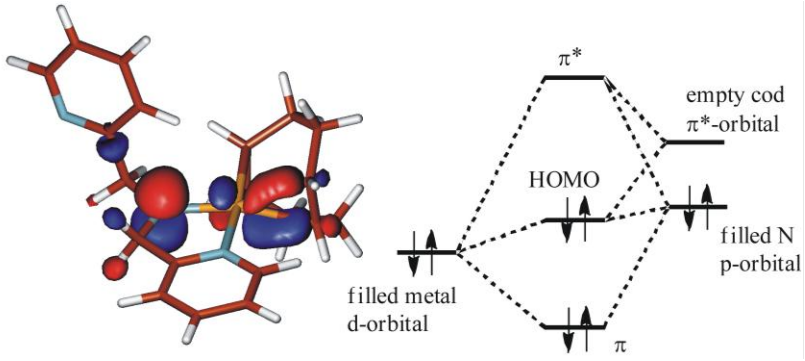

Figure 4. DFT calculated HOMO of the hypothetical Rh compound **5**, and a simplified MO scheme explaining the net π-bonding between Rh and the amido fragment. The HOMO of **2** is very similar.[18a]

While the above data hint to a better stabilisation of the {bpa–H}$^-$ ligand by iridium, it still does not provide a straightforward explanation why Rh complex **5** is not an isolable compound. Hence, to shed some more light on this problem, we performed some additional experiments and DFT calculations to investigate the equilibrium associated with the reactions shown in Scheme 6. Quite remarkably, reaction of the dinuclear iridium complex [(cod)Ir(bpa–2H)Ir(cod)] (**8**) with the free bpa ligand in toluene quantitatively produces the mononuclear complex [Ir(bpa–H)(cod)] (**2**, Scheme 6). However, no reaction of the dinuclear Rh complex [(cod)Rh(bpa–2H)Rh(cod)] (**7**) with bpa occurs at all even in a 1:5 ratio molar ratio at 60 ºC in C_6D_6 for 2 h. This means that the equilibrium shown in Scheme 6 lies almost entirely to the right for iridium (in black), while the corresponding equilibrium for the analogous Rh complexes lies almost entirely to the left (in red).

Scheme 6. Disproportionation/comproportionation equilibria between [M(cod)(bpa–H)] and [(cod)M(bpa–2H)M(cod)] + bpa. Relative energies (ΔE) of the equilibria were obtained with DFT calculations.

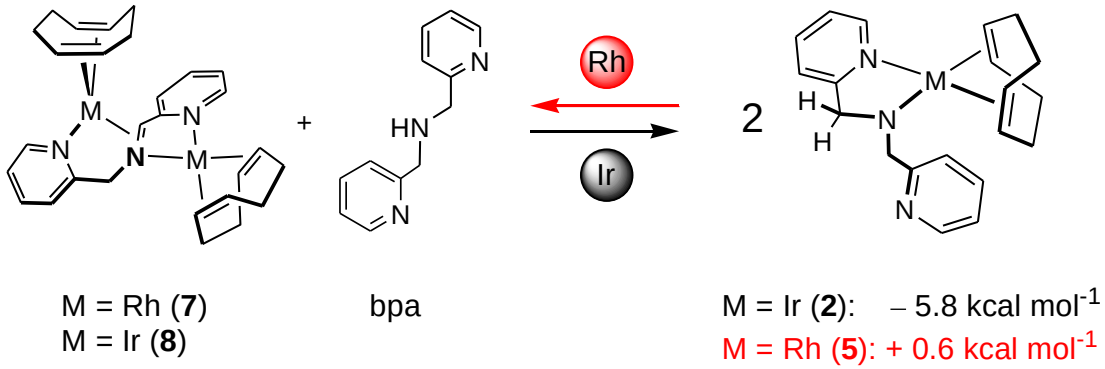

M = Rh (**7**)
M = Ir (**8**)

bpa

M = Ir (**2**): – 5.8 kcal mol^{-1}
M = Rh (**5**): + 0.6 kcal mol^{-1}

Because the metal in the imine compartment is best described being in the –I oxidation state (*vide supra*), the reaction in Scheme 6 is in fact an oxidative process in which one of the iridium atoms is being oxidized from Ir^{-I} to Ir^{I}. Since it is well know that the tendency to undergo oxidative processes is generally higher for the third row transition metals as compared to the second row transition metals, it is understandable that the equilibrium in Scheme 6 lies to the right for iridium while the corresponding equilibrium for the analogous rhodium complexes lies to the left. This provides a straightforward explanation for the fact that the amido rhodium complex **5** cannot be prepared, while the iridium analogue **2** is a stable compound.[40] It is clear that the amido rhodium complex **5** is thermodynamically unstable towards disproportionation, and readily forms the dinuclear complex **7** and the free bpa ligand. The thermodynamic differences are readily explained by a higher stability of the M^{-I} oxidation state in the dinuclear complexes for rhodium as compared to iridium. DFT calculations in the gas phase are in good qualitative agreement with these experimental observations (see Scheme 6). Therefore, the two above commented main reactions: $[M(bpa)(cod)]^{+}$ with KO^{t}Bu (1 molar-equivalent) and [(cod)M(bpa–2H)M(cod)] + bpa can be considered as proton coupled electron transfer reactions, with an acid/base component and a hidden redox process involving the reduction of one of the metals in the dinuclear entity. In this perspective, the expected acid/base behaviour prevails over the redox part for the

iridium complexes, while the redox process dominates over the acid/base contribution for the rhodium ones, and consequently, they undergo a cooperative reductive double deprotonation to the mixed-valence Rh^{-I},Rh^{I} compound.

Further experiments and DFT calculations clearly reveal that Rh feels most comfortable in the 'tetrahedral π-imine compartment', while Ir is most comfortable in the 'square planar' compartment. Reaction of [(cod)Rh(bpa–2H)Rh(cod)] (**7**) with [IrCl(cod)PPh_3] in C_6D_6 at 60°C produces almost quantitatively [(cod)Rh(bpa–2H)Ir(cod)] (**9**) and [RhCl(cod)PPh_3] (see also the Supporting Information). Thus, iridium replaces rhodium in the 'square-planar compartment' in this reaction. Similarly, reaction of [(cod)Ir(bpa–2H)Ir(cod)] (**8**) with [RhCl(cod)PPh_3] under the same conditions produces almost quantitatively **9** (and [IrCl(cod)PPh_3]). In this case, rhodium replaces iridium in the 'tetrahedral π-imine compartment' (Scheme 7).

Scheme 7. Replacing Rh by Ir in the 'square planar' compartment and replacing Ir by Rh in the 'tetrahedral compartment'.

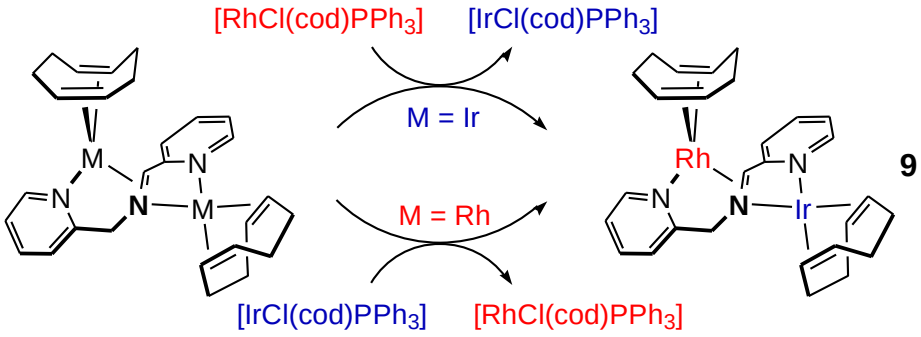

Moreover, reaction of the dinuclear Rh complex [(cod)Rh(bpa–2H)Rh(cod)] (**7**) with the dinuclear Ir complex [(cod)Ir(bpa–2H)Ir(cod)] (**8**) in C_6D_6 at 60°C produces almost quantitatively the heterodinuclear complex **9** (Scheme 8) instead of a statistical mixture of the complexes in a 1:2:1 ratio (see Supporting Information).

Scheme 8. Comproportionation of **7** and **8** to form two molecules of **9**. The relative energy (ΔE) for the comproportionation equilibrium was obtained with DFT calculations.

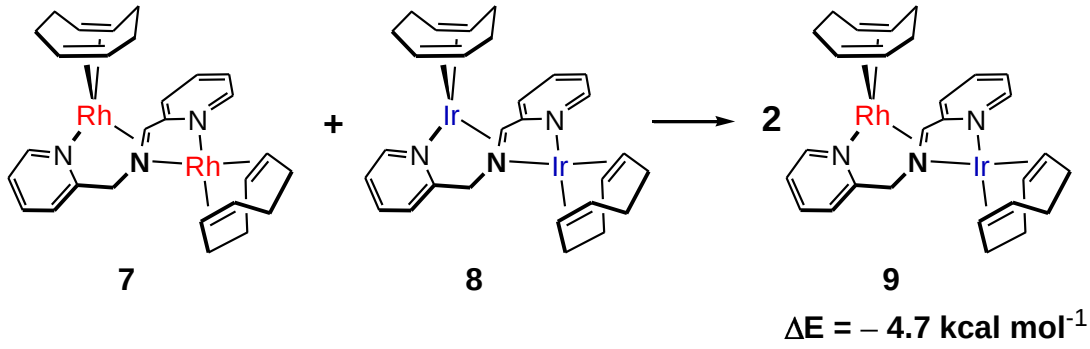

DFT calculations in the gas phase are in good qualitative agreement with these experiments. The comproportionation of **7** and **8** to **9** is exothermic by ~5 kcal mol^{-1} according to these calculations (Scheme 8). The calculations further reveal that the [(cod)Rh(bpa–2H)Ir(cod)] complex **9** with Rh in the 'tetrahedral π-imine compartment' and Ir in the 'square planar' compartment is ~4 kcal mol^{-1} more stable than the hypothetical [(cod)Ir^{-I}(bpa–2H)Rh^{I}(cod)] isomer **9'** with Ir in the 'tetrahedral π-imine compartment' and Rh in the 'square planar' compartment.

Oxygenation of complexes 7 and 8. In line with the electron rich nature of their metallate(–I) centers, the complexes **7** and **8** are very air-sensitive, and react rapidly with O_2 in benzene (Scheme 9). The reactions proceed with formation of the carboxamido complexes [M(bpam–H)(cod)] (M = Rh (**10**); Ir (**11**); bpam = N-(2-picolyl)picolinamide). Monitoring the reactions by NMR further revealed the formation of [{M(cod)(μ-OH)}$_2$] (M= Rh, Ir) in roughly equimolar amounts. These reactions are similar to those previously communicated for the Rh(nbd) analogs.[25] Complex **11** is also the result of the reaction of the anionic complex [**3**]$^-$ with oxygen.[18a]

Scheme 9. Oxygenation of **7** and **8** to form the carboxamido complexes **10** and **11**.

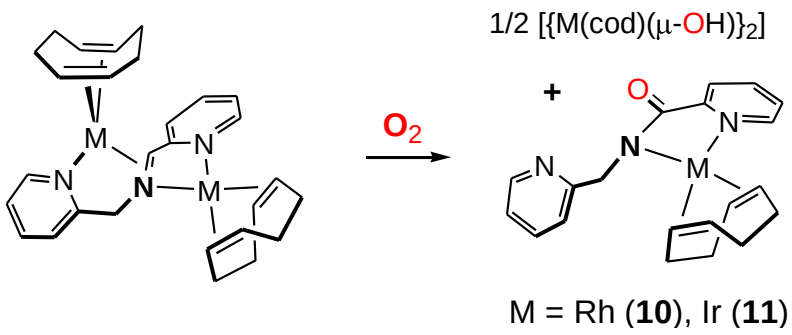

Complex **10** was identified by comparing its spectroscopic data with those of pure samples obtained from the reaction of [{M(cod)(μ-OMe)}$_2$] with bpam in diethyl ether (see Experimental Section). From these solutions, complex **10** was obtained as orange single crystals whose molecular structure is shown in Figure 5. Selected bond distances and angles are collected in Table 2.

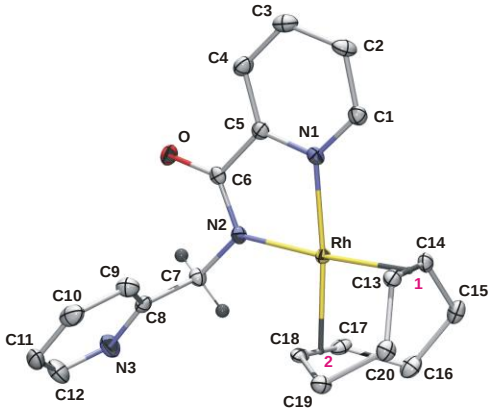

Figure 5. Molecular structure (ORTEP at 50% level) of complex **10**.

Coordination of the bpam–H ligand to rhodium in **10** occurs through the amido nitrogen (N2) and the nitrogen (N1) of the carbonyl-bound pyridyl ring. The square planar coordination geometry around rhodium is completed by the chelating cod ligand. The amido N2 and the carbon C6 are strictly planar (sum of the angles around the nitrogen Σ^0 = 359.8º [359.7º for the second independent molecule] and Σ^0 = 360.0º [360.0º] for the carbon. The five-membered metallacycle was found to be almost planar (the maximum deviation of the plane defined by Rh, N1, C5, C6, N2 is 0.019 Å [0.028 Å]). These data

clearly reflect a sp^2-hybridization for the N2 and C6 atoms. In addition, the N1–C5 and N2–C6 distances are ca. 0.15 Å shorter than C5–C6, pointing to a single bond between the carbon atoms and some multiple bond character for both C–N bonds.

Table 2. Selected bond distances (Å) for complex **10**.

Rh–N1	2.095(3) [2.144(3)]	N1–C1	1.342(4) [1.342(4)]
Rh–N2	2.059(2) [2.051(2)]	C1–C2	1.387(4) [1.380(4)]
Rh–Ct1[a]	2.013() [2.012(3)]	C2–C3	1.379(5) [1.384(4)]
Rh–Ct2[a]	2.015() [2.016(3)]	C3–C4	1.389(5) [1.384(4)]
C13–C14	1.403(4) [1.389(3)]	C4–C5	1.382(4) [1.382(4)]
C17–C18	1.383(4) [1.395(3)]	C5–N1	1.348(4) [1.348(4)]
C5–C6	1.509(4) [1.498(4)]	C6–O	1.243(4) [1.246(3)]
C6–N2	1.340(4) [1.336(4)]	N2–C7	1.457(4) [1.456(4)]

[a] Ct1 and Ct2 are the middle points between C13 and C14 and C17 and C18, respectively. In brackets the data for the second independent molecule.

The formation and isolation of the rhodium carboxamido compound **10** is in sharp contrast with the thermodynamic instability of the (structurally and electronically similar) amido complex **5**. Delocalization of the lone pair of N2 to the adjacent carbonyl (partly removing its π-interactions with the filled metal-d_π-orbitals) and the inability of **10** to host another metal atom are the most likely explanations for this different behavior.[41]

Summary and Conclusions

Deprotonation of $[Ir^I(bpa)(cod)]^+$ complex with 1 molar equivalent of a strong base leads to quantitative formation of the neutral mono-deprotonated and mononuclear $[Ir^I(bpa–H)(cod)]$ (**2**) species. All attempts to prepare the $[Rh^I(bpa–H)(cod)]$ analog led to spontaneous *cooperative reductive double deprotonation* of the $[Rh^I(bpa)(cod)]^+$ complex, thus producing the Rh^{-I},Rh^I mixed-valence

[(cod)Rh^{-I}(bpa–2H)Rh^{I}(cod)] (**7**) species. The dinuclear iridium analog **8** can be prepared, but is unstable in the presence of 1 molar equivalent of the free bpa ligand leading to quantitative formation of **2**. Hence, for iridium the spontaneity of the process ([**8**] + bpa → 2 [**2**]) is reversed from that occurring for rhodium (2 [**5**] → [**7**] + bpa). These thermodynamic differences are readily explained by a lower stability of the M^{-I} oxidation state for iridium as compared to rhodium in the dinuclear complexes **8** and **7**. Formation of two equivalents of [Ir^{I}(bpa–H)(cod)] from **8** and free bpa is an *oxidative* process, which is favorable for iridium. Disproportionation of [Rh^{I}(bpa–H)(cod)] into **7** and free bpa is a *reductive* process, which is favorable for rhodium. The observed reductive deprotonation process leads to highly unusual structures and unexpected reactivities, which underlines the general importance of the substantial effect of 'redox non-innocent ligands' on the electronic structure and catalytic activity of transition metals.[42]

Experimental Section

General methods. All procedures were performed under an argon or N_2 atmosphere, using standard Schlenk techniques. Solvents were dried and distilled under argon before use by standard methods.[43] NMR experiments were carried out on Bruker AV 500, AV 400, and DPX 200 spectrometers operating at 500, 400, and 200 MHz for ^{1}H, respectively. Chemical shifts are reported in ppm and referenced to $SiMe_4$, using the internal signal of the deuterated solvent as reference. The bpa numbering for the complexes correspond to that in Figure 3 for **7**. The complexes [{M(cod)(μ-OMe)}$_2$],[44] [Ir(bpa)(cod)]PF_6 ([**1**]$^+$)[17] and [Rh(bpa)(cod)]PF_6 ([**4**]$^+$)[21a] were prepared according to the literature descriptions. All other chemicals are commercially available and were used without further purification.

[(cod)Rh(bpa–2H)Rh(cod)] (7). Liquid bis(2-picolyl)amine (dpa, 97%) (55.7 μL, 0.31 mmol) was added to a yellow suspension of [{Rh(cod)(μ-OMe)}$_2$] (150.0 mg, 0.31 mmol) in 10 mL of diethyl ether. After stirring for 15 min, the resulting dark-red/brown solution was concentrated to ca. 7 mL, layered with pentane (10 mL), and left in the fridge (4 ºC) overnight. The mother liquor was decanted, and the

solid was washed with pentane (2 x 5mL), and vacuum-dried. Yield: 147.1 mg (77%). Crystals suitable for X-ray diffraction resulted by layering with hexane the ethereal red-brown solution mentioned above. ^{1}H NMR (500 MHz, C_6D_6, 25 ºC): δ 8.76 (br d, J = 4.2 Hz, 1H, H^{A1}), 7.15 (d, J = 7.6 Hz, 1H, H^{A4}), 7.01 (td, J = 7.6, 1.7 Hz, 1H, H^{A3}), 6.80 (d, J = 6.5 Hz, 1H, H^{B1}), 6.58 (m, 2H, H^{B3} and H^{A2}), 6.20 (d, J = 8.5 Hz, 1H, H^{B4}), 5.78 (td, J = 6.5, 1.2 Hz, 1H, H^{B2}), 4.75 (m, 2H, H^{21}), 4.33 (s, 1H, HC=N), 4.22 (δ_A, 1H) and 4.12 (δ_B, $J_{A,B}$ = 17.0 Hz, 1H, CH_2), 4.04 (m, 1H, H^{11}), 3.70 (m, 3H, H^{12}, H^{15} and H^{16}), 3.41 (m, 2H, H^{22}), 2.71 (m, 1H, H^{14a}), 2.53 (m, 2H, H^{24a}), 2.47 (m, 1H, H^{18a}), 2.40 (m, 1H, H^{13a}), 2.31 (m, 1H, H^{17a}), 2.16 (m, 2H, H^{24b}), 2.12 (m, 2H, H^{23a}), 2.05 (m, 1H, H^{14b}), 2.01 (m, 1H, H^{18b}), 1.81 (m, 2H, H^{23b}), 1.77 (m, 1H, H^{17b}), 1.71 (m, 1H, H^{13b}). ^{13}C{^{1}H} NMR (125 MHz, C_6D_6, 25 ºC): δ 162.2 (C^{A5}), 149.2 (C^{A1}), 148.5 (C^{B5}), 143.0 (C^{B1}), 135.6 (C^{A3}), 130.6 (C^{B3}), 121.4 (C^{A2}), 121.0 (C^{A4}), 115.5 (C^{B4}), 110.1 (C^{B2}), 82.2 (d, $J_{C,Rh}$ = 7 Hz, HC=N), 79.1 (d, $J_{C,Rh}$ = 14 Hz, C^{11}), 76.2 (d, $J_{C,Rh}$ = 13 Hz, C^{15}), 73.9 (d, $J_{C,Rh}$ = 12 Hz, C^{12}), 73.1 (d, $J_{C,Rh}$ = 12 Hz, C^{16}), 72.7 (d, $J_{C,Rh}$ = 14 Hz, C^{22}), 67.1 (d, $J_{C,Rh}$ = 14 Hz, C^{21}), 60.5 (CH_2), 33.6 (C^{24}), 32.7 (C^{18}), 31.7 (C^{14}), 31.2 (C^{23}), 30.5 (C^{17}), 29.6 (C^{13}). Anal. Calcd. (Found) for $C_{28}H_{35}N_3Rh_2$ (619.4): C, 54.29 (54.18); H, 5.69 (5.60); N, 6.78 (6.84).

Alternatively, complex **7** can be prepared as follows in thf: Solid KO^{t}Bu (62.0 mg, 0.55 mmol) was added to a yellow solution of [**4**]PF_6 (278.0 mg, 0.50 mmol) in 10 mL of thf. An immediate colour change to purple-brown was observed as a 1:1 mixture of bpa and **7** was obtained. The resulting mixture (**7** contaminated with KPF_6) was evaporated, washed with pentane, dried under vacuum, and was directly analysed by NMR. ^{1}H NMR (200 MHz, thf-d_8, 25 ºC): δ 8.81 (d, J = 5 Hz, 1H, H^{A1}), 7.63 (m, 1H, H^{A3}), 7.33 (d, J = 8 Hz, 1H, H^{A4}), 7.11 (m, 1H, H^{A2}), 6.96 (m, 2H, H^{B1} and H^{B3}), 6.48 (d, J = 8 Hz, 1H, H^{B4}), 6.11 (m, 1H, H^{B2}), 4.48 (m, 2H, cod-CH), 4.19 (s, 1H, C*H*=N), 4.16 (δ_A, 1H) and 3.99 (δ_B, $J_{A,B}$ = 17 Hz, 1H, CH_2), 3.68 (br s, 3H, cod-C*H*=), 3.01 (m, 2H, cod-C*H*=), 2.64 (m, 2H, cod-CH_2), 2.44 (m, 5H, cod-CH_2 and cod-C*H*=), 1.95 (m, 8H, cod-CH_2), 1.57 (m, 2H, cod-CH_2). ^{13}C{^{1}H} NMR (50 MHz, thf-d_8, 25 ºC): δ 162.91 (C^{A5}), 150.99 (C^{A1}), 144.08 (C^{B1}), 137.13 (C^{A3}), 132.17 (C^{B3}), 122.90 (C^{A2}), 122.18 (C^{A4}), 116.69 (C^{B4}), 111.48 (C^{B2}), 81.88 (d, $J_{C,Rh}$ = 8 Hz, *C*H=N), 82.29 (d, $J_{C,Rh}$ = 13 Hz,

cod-C*H*=), 79.12 (d, $J_{C,Rh}$ = 12 Hz, cod-C*H*=), 76.51 (d, $J_{C,Rh}$ = 12 Hz, cod-C*H*=), 75.54 (d, $J_{C,Rh}$ = 14 Hz, cod-C*H*=), 73.01 (d, $J_{C,Rh}$ = 14 Hz, cod-C*H*=), 66.98 (d, $J_{C,Rh}$ = 14 Hz, cod-C*H*=), 61.23 (-*C*H_2-), 34.58 (cod-CH_2), 33.47 (cod-CH_2), 32.40 (cod-CH_2), 31.81 (cod-CH_2), 31.54 (cod-CH_2), 30.57 (cod-CH_2).

[(cod)Ir(bpa–2H)Ir(cod)] (8) can be prepared as described for **7** starting from bis(2-picolyl)amine (bpa, 97%) (45.1 μL, 0.23 mmol) and [{Ir(cod)(μ-OMe)}$_2$] (150.0 mg, 0.23 mmol). Yield: 153.5 mg (85%). Crystals suitable for X-ray diffraction resulted by layering with hexane the ethereal red-brown solution mentioned above. ^{1}H NMR (500 MHz, C_6D_6, 25 ºC): δ 9.10 (br d, J = 5.3 Hz, 1H, H^{A1}), 7.52 (br d, J = 5.6 Hz, 1H, H^{B1}), 6.73 (td, J = 8.4, 1.3 Hz, 1H, H^{B3}), 6.71 (td, J = 7.7, 1.4 Hz, 1H, H^{A3}), 6.44 (d, J = 8.4 Hz, 1H, H^{B4}), 6.37 (d, J = 7.7 Hz, 1H, H^{A4}); 6.21 (td, J = 7.7, 1.1 Hz, 1H, H^{A2}), 5.79 (td, J = 8.4, 1.2 Hz, 1H, H^{B2}), 4.20 (m, 1H, H^{16}), 4.07 (δ_A, 1H) and 3.98 (δ_B, $J_{A,B}$ = 17.2 Hz, 1H, CH_2), 4.04 (m, 2H, H^{21}), 3.95 (m, 1H, H^{15}), 3.54 (m, 1H, H^{12}), 3.42 (m, 1H, H^{11}), 3.30 (s, 1H, HC=N), 3.09 (m, 2H, H^{24a}), 2.78 (m, 2H, H^{24b}), 2.71 (m, 1H, H^{17a}), 2.67 (m, 1H, H^{18a}), 2.55 (m, 1H, H^{14a}), 2.49 (m, 1H, H^{13a}), 2.16 (m, 2H, H^{23a}), 2.11 (m, 2H, H^{22}), 1.96 (m, 1H, H^{14b}), 1.94 (m, 1H, H^{18b}), 1.91 (m, 1H, H^{13b}), 1.81 (m, 1H, H^{17b}), 1.38 (m, 2H, H^{23b}). ^{13}C{^{1}H} NMR (125 MHz, C_6D_6, 25 ºC): δ 175.4 (C^{B5}), 163.9 (C^{A5}), 153.1 (C^{A1}), 143.3 (C^{B1}), 133.7 (C^{A3}), 132.9 (C^{B3}), 122.0 (C^{A2}), 121.7 (C^{A4}), 117.4 (C^{B4}), 114.4 (C^{B2}), 71.9 (HC=N), 65.2 (C^{15}), 60.8 (CH_2), 59.6 (C^{12}), 55.2 (C^{11}), 55.1 (C^{16}), 53.2 (C^{22}), 48.5 (C^{21}), 40.0 (C^{24}), 33.0 (C^{14}), 32.5 (C^{13}), 32.0 (C^{17}), 31.4 (C^{18}), 30.3 (C^{23}). Anal. Calcd. (Found) for $C_{28}H_{35}N_3Ir_2$ (798.0): C, 42.14 (42.25); H, 4.42 (4.31); N, 5.26 (5.54).

Alternatively, complex **8** can be prepared as follows: Two equivalents of KO^{t}Bu (0.123 g, 1.1 mmol) were added to the light yellow solution of [**1**]PF_6 (0.323 g, 0.50 mmol) in 10 ml of thf. [{Ir(μ-Cl)(cod)}$_2$] (0.099 g ,0.2 mmol) was added to the resulting red-brown solution. The resulting mixture (**8** still contaminated with KPF_6 and KCl salts) was evaporated, washed with pentane, dried in vacuo and was directly analysed by NMR. ^{1}H NMR (200 MHz, thf-d_8, 25 ºC): δ 9.17 (d, J = 5 Hz, 1H, H^{A1}), 7.57 (m, 2H, H^{A3} and H^{B1}), 7.27 (m, 2H, H^{A4} and H^{B3}), 7.01 (t, J = 6 Hz, 1H, H^{A2}), 6.73 (d, J = 8 Hz, 1H,

H^{B4}), 6.31 (m, 1H, H^{B2}), 4.27 (m, 2H, -CH_2-), 4.01 (m, 2H, cod-C*H*=), 3.84 (m, 2H, cod-C*H*=), 3.36 (m, 2H, cod-C*H*=), 3.30 (s, 1H, C*H*=N), 3.20 (m, 2H, cod-C*H*=), 2.72 (m, 4H, cod-CH_2), 2.43-2.24 (m, 2H, cod-CH_2), 2.0–1.5 (m, 10H, cod-CH_2). $^{13}C\{^1H\}$ NMR (50 MHz, thf-d_8, 25 ºC): δ 176.2 (C^{B5}), 164.9 (C^{A5}), 153.7 (C^{A1}), 144.0 (C^{B1}), 135.2 (C^{A3}), 133.7 (C^{B3}), 123.1 (C^{A2}), 121.06 (C^{A4}), 118.1 (C^{B4}), 114.9 (C^{B2}) 71.9 (*CH*=N), 65.4 (cod-C*H*=), 61.2 (-*C*H_2-), 59.7 (cod-C*H*=), 55.1 (cod-C*H*=), 54.9 (cod-C*H*=), 53.0 (cod-C*H*=), 48.1 (cod-C*H*=), 40.2 (cod-CH_2), 33.1 (cod-CH_2), 32.8 (cod-CH_2), 32.2 (cod-CH_2), 31.6 (cod-CH_2), 30.2 (cod-CH_2).

[(cod)Rh(bpa−2H)Ir(cod)] (9). To a solution of [Ir(bpa−H)(cod)] (50.0 mg, 0.10 mmol) in toluene (3 mL) solid [{Rh(cod)(μ-OMe)}$_2$] (24.3 mg, 0.05 mmol) was added. After stirring for 15 min, hexane (8 mL) was added. The dark-brown solid that precipitated was filtered off, washed with hexane and vacuum-dried. Yield: 55.1 mg (77.5 %). ^1H NMR (500 MHz, C_6D_6, 25 ºC): δ 8.51 (ddd, *J* = 4.9, 1.7, 0.8 Hz, 1H, H^{A1}), 7.43 (d, *J* = 7.9 Hz, 1H, H^{A4}), 7.06 (td, *J* = 7.7, 1.8 Hz, 1H, H^{A3}), 7.01 (d, *J* = 6.6 Hz, 1H, H^{B1}), 6.60 (dd, *J* = 6.7, 5.0 Hz, 1H, H^{A2}), 6.50 (ddd, *J* = 8.6, 6.5, 1.1 Hz, 1H, H^{B3}), 6.36 (d, *J* = 8.7 Hz, 1H, H^{B4}), 5.78 (td, *J* = 6.6, 1.4 Hz, 1H, H^{B2}), 5.62 (s, 1H, HC=N), 4.72 (δ_A, 1H) and 4.58 (δ_B, $J_{A,B}$ = 16.5 Hz, 1H) (CH_2 bpa), 4.08 (br, 2H, =CH, Rh(cod)), 3.91 (m, 1H, =CH, Ir(cod)), 3.54 (br, 2H, =CH, Rh(cod)), 3.40 (m, 2H, =CH, Ir(cod)), 3.25 (m, 1H, =CH, Ir(cod)), 2.52 (m, 1H, CH_2, Ir(cod)), 2.33 (m, 5H, CH_2, Ir(cod)), 2.01 (m, 2H, CH_2, Rh(cod)), 1.91 (m, 2H, CH_2, Rh(cod)), 1.83 (m, 1H, CH_2, Ir(cod)), 1.74 (m, 5H, 4 from CH_2, Rh(cod) and 1 from CH_2, Ir(cod)). $^{13}C\{^1H\}$ NMR (125 MHz, C_6D_6, 25 ºC): δ 161.9 (C^{A5}), 149.1 (C^{A1}), 141.5 (C^{B1}), 136.4 (C^{A3}), 134.6 (C^{B5}), 128.1 (C^{B3}), 121.6 (C^{A2}), 121.1 (C^{A4}), 116.5 (C^{B4}), 110.3 (C^{B2}), 92.7 (d; $J_{Rh,C}$ = 5.1 Hz; HC=N), 73.7 (d, $J_{Rh,C}$ = 14.7 Hz) and 72.3 (d, $J_{Rh,C}$ = 13.7 Hz) (=CH, Rh(cod)), 62.6, 58.7, 56.9 and 56.4, (=CH, Ir(cod)), 60.7 (CH_2 bpa), 34.6, 33.4, 31.1 and 30.4 (CH_2, Ir(cod)), 32.0 and 31.6 (CH_2, Rh(cod)). Anal. Calcd. (Found) for $C_{28}H_{35}N_3IrRh$ (708.7): C, 47.45 (47.37); H, 4.98 (4.87); N, 5.93 (5.76).

Alternatively, complex **9** can also be prepared in a similar way as described for the synthesis of **8** in thf, using [{Rh(μ-Cl)(cod)}$_2$] instead of [{Ir(μ-Cl)(cod)}$_2$]. ^1H NMR (200 MHz, thf-d_8, 25 ºC): δ 8.49

(d, J = 5 Hz, 1H, H^{A1}), 7.62 (t, J = 7 Hz, 1H, H^{A3}), 7.42 (d, J = 8 Hz, 1H, H^{A4}), 7.10 (m, 2H, H^{A2} and H^{B1}), 6.92 (m, 2H, H^{B4} and H^{B2}), 6.18 (m, 1H, H^{B3}), 6.02 (s, 1H, C*H*=N), 4.36 (m, 4H, cod-C*H*= and -CH_2-), 3.71 (m, 2H, cod-C*H*=), 3.56 (m, 2H, cod-C*H*=), 3.29 (m, 2H, cod-C*H*=), 2.02 (m, 16H, cod-CH_2). $^{13}C\{^1H\}$ NMR (50 MHz, thf-d_8, 25 ºC): δ 162.1 (C^{A5}), 149.6 (C^{A1}), 141.9 (C^{B1}), 137.0 (C^{A3}), 136.3 (C^{B5}), 129.1 (C^{B3}), 122.2 (C^{A4}), 121.6 (C^{A2}), 117.3 (C^{B4}), 111.1 (C^{B2}), 93.1 (d, $J_{C,Rh}$ = 5 Hz, C*H*=N), 72.6 (d, $J_{C,Rh}$ = 14 Hz, cod-C*H*=), 70.8 (d, $J_{C,Rh}$ = 14 Hz, cod-C*H*=), 62.6 (cod-C*H*=), 60.9 (-CH_2-), 58.7 (cod-C*H*=), 56.8 (cod-C*H*=), 56.4 (cod-C*H*=), 34.8 (cod-CH_2), 33.6 (cod-CH_2), 32.4 (cod-CH_2), 31.9 (cod-CH_2), 31.5 (cod-CH_2), 30.8 (cod-CH_2).

[Rh(bpam−H)(cod)] (10). Solid *N*-(2-picolyl)picolinamide (bpam) (134.3 mg, 0.63 mmol) was added to a solution of [{Rh(cod)(μ-OMe)}$_2$] (150.0 mg, 0.31 mmol) in toluene (5 mL). An immediate orange solution was formed after mixing the reagents. The solution was evaporated to ca. 2 mL, layered with hexane (10 mL) and kept undisturbed in the freezer at –30 ºC overnight to render orange crystals, which were washed with cold hexane (3 x 3 mL) and vacuum-dried. Yield: 223.7 mg (85 %). ^{1}H NMR (400 MHz, C_6D_6, 25 ºC): δ 8.53 (ddd, J = 4.8, 1.8, 0.9 Hz, 1H, H^{A1}), 8.09 (ddd, J = 7.8, 1.5, 0.7 Hz, 1H, H^{B4}), 7.92 (d, J = 7.9 Hz, 1H, H^{A4}), 7.15 (td, J = 7.7, 1.8 Hz, 1H, H^{A3}), 6.87 (d, J = 5.3 Hz, 1H, H^{B1}), 6.83 (td, J = 7.7, 1.5 Hz, 1H, H^{B3}), 6.62 (ddd J = 7.4, 4.8, 1.1 Hz, 1H, H^{A2}), 6.24 (ddd, J = 7.3, 5.3, 1.5 Hz, 1H, H^{B2}), 4.92 (s, 2H, CH_2^{bpam}), 4.60 (m, 2H) and 3.50 (m, 2H), HC= (cod), 2.19 (m, 4H, CH_2^{exo} (cod)), 1.65 (m, 4H, CH_2^{endo} (cod)). $^{13}C\{^1H\}$ NMR (100 MHz, C_6D_6, 25 ºC): δ 173.2 (d, $J_{C,Rh}$ = 1.5 Hz, CO), 163.2 (C^{A5}), 157.3 (C^{B5}), 148.9 (C^{A1}), 144.3 (C^{B1}), 138.8 (C^{B3}), 135.9 (C^{A3}), 125.3 (C^{B2}), 125.2 (C^{B4}), 123.0 (C^{A4}), 121.1 (C^{A2}), 84.1 (d, $J_{C,Rh}$ = 12.9 Hz) and 77.0 (d, $J_{C,Rh}$ = 12.1 Hz; HC= (cod), 51.1 (d, $J_{C,Rh}$ = 1.5 Hz, CH_2^{bpam}), 31.3 and 30.4 CH_2 (cod). Anal. Calcd. (Found) for $C_{20}H_{22}N_3ORh$ (423.3): C, 56.74 (56.81); H, 5.24 (5.11); N, 9.93 (9.91).

[Rh(bpa)(cod)][RhCl$_2$(cod)] was independently prepared as follows: bis(2-picolyl)amine (bpa, 97%) (37.5 μL, 0.21 mmol) was added to a solution of [{Rh(μ-Cl)(cod)}$_2$] (100.0 mg, 0.21 mmol) in toluene (5 mL). The initial yellow solution turned pale green while a yellow solid started to precipitate. After

stirring for 30 min the liquor mother was decanted and the solid was washed with diethyl ether (2 x 5 mL) and vacuum-dried. Yield: 123.5 mg (88 %). ^{1}H NMR (400 MHz, CD_2Cl_2, 25 ºC): δ 8.63 (d, J = 4.5 Hz, 2H, H^{A1}), 7.59 (t, J = 7.4 Hz, 2H, H^{A3}), 7.21 (d, J = 6.6 Hz, 2H, H^{A4}), 7.16 (t, J = 7.4 Hz, 2H, H^{A2}), 6.53 (br t, J = 4.2 Hz, 1H, NH), 4.54 (s, 4H, CH_2^{bpa}), 4.18 (br s, 4H, HC=), 2.39 (br s, 4H, CH_2^{exo}) and 1.59 (br s, 4H, CH_2^{exo}; (cod^A), 3.85 (br s, 4H, HC=), 2.57 (br s, 4H, CH_2^{exo}) and 1.86 (br s, 4H, CH_2^{exo}; (cod^B) [cod^A is that bonded to the anion while cod^B is that bonded to the cation]. Anal. Calcd. (Found) for $C_{28}H_{37}N_3Cl_2Rh_2$ (692.3): C, 48.58 (48.38); H, 5.39 (5.55); N, 6.07 (6.20).

Reaction of [(cod)Rh(bpa−2H)Rh(cod)] (7) with [(cod)Ir(bpa−2H)Ir(cod)] (8). Solid [(cod)Rh(bpa−2H)Rh(cod)] (**7**) (4.8 mg, 7.8 x 10^{-3} mmol) and [(cod)Ir(bpa−2H)Ir(cod)] (**8**) (6.2 mg, 7.8 x 10^{-3} mmol) were introduced in a NMR tube and C_6D_6 (0.5 mL) was added. Evolution of the mixture was monitorized by ^{1}H NMR at 60 ºC. NMR data indicate the clean and almost quantitative formation of complex [(cod)Rh(bpa−2H)Ir(cod)] (**9**) after 2h heating (see Supporting Information).

Reaction of [(cod)Rh(bpa−2H)Rh(cod)] (7) with [IrCl(cod)(PPh$_3$)]. Solid [(cod)Rh(bpa−2H)Rh(cod)] (**7**) (6.0 mg, 9.7 x 10^{-3} mmol) and [IrCl(cod)(PPh_3)] (5.8 mg, 9.7 x 10^{-3} mmol) were introduced in an NMR tube and C_6D_6 (0.5 mL) was added. Evolution of the mixture was monitored by ^{1}H NMR at 60 ºC. The NMR data indicate the clean and almost quantitative formation of [(cod)Rh(bpa−2H)Ir(cod)] (**9**) and [RhCl(cod)(PPh_3)] after 50 min heating (see Supporting Information).

Reaction of [(cod)Ir(bpa−2H)Ir(cod)] (8) with [RhCl(cod)(PPh$_3$)]. Solid [(cod)Ir(bpa−2H)Ir(cod)] (**8**) (6.0 mg, 7.5 x 10^{-3} mmol) and [RhCl(cod)(PPh_3)] (3.8 mg, 7.5 x 10^{-3} mmol) were introduced in a NMR tube and C_6D_6 (0.5 mL) was added. Evolution of the mixture was monitored by ^{1}H NMR at 60 ºC. The NMR data indicate the clean and almost quantitative formation of [(cod)Rh(bpa−2H)Ir(cod)] (**9**) and [IrCl(cod)(PPh_3)] after 50 min heating.

DFT geometry optimizations. The geometry optimizations were carried out with the Turbomole program[45a,b] coupled to the PQS Baker optimizer.[46] Geometries were fully optimized as minima at the ri-DFT BP86[47] level using the Turbomole SV(P) basis set[45c,d] on all atoms (small-core

pseudopotentials[45c,e] on Rh and Ir). Broken symmetry calculations were performed at the DFT b3-lyp,[48] def-TZVP[45c,f] of theory. Orbitals were visualized with the Molden program.[49]

X-ray diffraction studies on 7·0.5(C_6H_{14}), 8·0.5(C_6H_{14}), and 10. Selected crystallographic data for the three complexes can be found in Table S1 (Supporting information). Intensity measurements were collected with a Smart Apex diffractometer, with graphite-monochromated MoK_α radiation. A semi-empirical absorption correction was applied to each data set, with the multi-scan[50] methods. All non-hydrogen atoms were refined with anisotropic temperature factors except those corresponding to the disordered hexane solvent (complexes **7** and **8**), which were refined with fixed isotropic thermal parameters. The hydrogen atoms were placed at calculated positions, with the exception of the olefinic cod protons and the methine HC=N proton which were found on the Fourier map. They were refined isotropically in riding mode. The structures were solved by the Patterson method and refined by full-matrix least-squares with the program SHELX97[51] in the WINGX[52] package. Two independent molecules were found for complex **10**.

Acknowledgment. This research was supported by the MICINN/FEDER (Project CTQ2008-03860, Spain) and Gobierno de Aragón (GA, Project PI55/08, Spain), the Netherlands Organization for Scientific Research (NWO-CW VIDI project 700.55.426), the European Research Council (ERC, EU 7th framework program, grant agreement 202886-CatCIR), and the University of Amsterdam. M. P. del Río and L. Asensio thank GA and MICINN/FEDER, respectively, for a fellowship.

Supporting Information Available. ORTEP of complex **8**, selected NMR spectra of complexes **8**-**10**, monitoring of selected reactions by ^1H and $^{31}P\{^1H\}$ NMR, selected crystal, measurement and refinement data for compounds **7**, **8** and **10**, and CIF files for these compounds. This material is free of charge via the Internet at http://pubs.acs.org.

REFERENCES

(1) (a) Noyori, R.; Ohkuma, T. *Angew. Chem. Int. Ed.* **2001**, *40*, 40−73; (b) short review: Muñiz, K. *Angew. Chem. Int. Ed.* **2005**, *44*, 6622−6627.

(2) See for example: (a) Wu, X.; Wang, C.; Xiao, J. *Platinum Metals Rev.* **2010**, *54*, 3−19 *and references therein*; (b) Li, X.; Li, L.; Tang, Y.; Zhong, L.; Cun, L.; Zhu, J.; Liao, J.; Deng, J. *J. Org. Chem.* **2010**, *75*, 2981−2988; (c) Tang, Y.; Xiang, J., Cun, L., Wang, Y.; Shu, J.; Liao, J.; Deng, J. *Tetrahedron Asymmetr.* **2010**, *21*, 1900−1905; (d) Blaker, A. J.; Duckett, S. B.; Grace, J.; Perutz, R. N.; Whitwood, A. C. *Organometallics* **2009**, *28*, 1435−1446; (e) Blacker, A. J.; Clot, E.; Duckett, S. B.; Eisenstein, O.; Grace, J.; Nova, A.; Perutz, R. N.; Taylor, D. J.; Whitwood, A. C. *Chem. Commun.* **2009**, 6801−6803; (f) Arita, S.; Koike, T.; Kayaki, Y.; Ikariya, T. *Chem. Asian J.* **2008**, *3*, 1479−1485.

(3) (a) Zweifel, T.; Naubron, J.; Büttner, T.; Ott, T.; Grützmacher, H. *Angew. Chem. Int. Ed.*, **2008**, *47*, 3245−3249; (b) Maire, P.; Büttner, T.; Breher, F.; Le Floch, P.; Grützmacher, H. *Angew. Chem. Int. Ed.* **2005**, *44*, 6318−6323.

(4) Ishiwata, K.; Kuwata, S.; Ikariya, T. *J. Am. Chem. Soc.* **2009**, *131*, 5001−5009.

(5) (a) Tye, J. W.; Hartwig, J. F. *J. Am. Chem. Soc.* **2009**, *131*, 14703−14712; (b) Zhao, P.; Krug, C.; Hartwig, J. F. *J. Am. Chem. Soc.* **2005**, *127*, 12066−12073; (c) Brunet, J.-J.; Commenges, G.; Neibecker, D.; Philippot, K. *J. Organomet. Chem.* **1994**, *469*, 221−228.

(6) Takemoto, S.; Otsuki, S.; Hashimoto, Y.; Kamikawa, K.; Matsuzaka, H. *J. Am. Chem. Soc.* **2008**, *130*, 8904−8905.

(7) Tejel, C.; Ciriano, M. A.; López, J. A.; Jiménez, S.; Bordonaba, M.; Oro, L. A. *Chem. Eur. J.* **2007***, 13***,** 2044−2053.

(8) Retboll, M.; Ishii, Y.; Hidai, M. *Chem. Lett.* **1998***,* 1217–1218.

(9) (a) Tejel, C.; Ciriano, M. A.; Bordonaba, M.; López, J. A.; Lahoz, F. J.; Oro, L. A. *Chem. Eur. J.* **2002**, *8*, 3128–3138; (b) Tejel, C.; Ciriano, M. A.; Bordonaba, M.; López, J. A.; Lahoz, F. J.; Oro, L. A. *Inorg. Chem.* **2002**, *41*, 2348–2355.

(10) Oro, L. A.; Ciriano, M. A.; Tejel, C.; Bordonaba, M.; Graift, C.; Tiripicchio, A. *Chem. Eur. J.* **2004**, *10*, 708–715.

(11) (a) Dzik, W. I.; Arruga, L. F.; Siegler, M. A.; Spek, A. L.; Reek, J. N. H.; de Bruin, B. *Organometallics* **2011**, *30*, 1902–1913; (b) Tejel, C.; Ciriano, M. A.; Passarelli, V.; López, J. A.; de Bruin, B. *Chem. Eur. J.* **2008**, *14*, 10985–10998; (c) Connelly, N. G.; Loyns, A. C.; Fernández, M. J.; Modrego, J.; Oro, L. A. *J. Chem. Soc.; Dalton Trans.* **1989**, 683–687.

(12) (a) Sharp, P. R. *J. Chem. Soc., Dalton Trans.* **2000**, 2647–2657; (b) Ge, Y.-W.; Ye, Y.; Sharp, P. R. *J. Am. Chem. Soc.* **1994**, *116*, 8384–8385.

(13) Büttner, T.; Geier, J.; Frison, G.; Harmer, J.; Calle, C.; Schweiger, A.; Schönberg, H.; Grützmacher, H. *Science* **2005**, *307*, 235–238.

(14) (a) Maire, P.; Königsmann, M.; Sreekanth, A.; Harmer, J.; Schweiger, A.; Grützmacher, H. *J. Am. Chem. Soc.* **2006**, *128*, 6578−6580.

(15) (a) Hetterscheid, D. G. H.; Kaiser, J.; Reijerse, E. J.; Peters, T. P. J.; Thewissen, S.; Blok, A. N. J.; Smits, J. M. M.; de Gelder, R.; de Bruin, B. *J. Am. Chem. Soc.* **2005**, *127*, 1895–1905; (b) Hetterscheid, D. G. H.; Bens, M.; de Bruin, B. *Dalton Trans.* **2005**, 979–984.

(16) Hetterscheid, D. G. H.; Klop, M.; Kicken, R. J. N. A. M.; Smits, J. M. M.; Reijerse, E. J.; de Bruin, B. *Chem. Eur. J.* **2007**, *13*, 3386–3405.

(17) Hetterscheid, D. G. H.; de Bruin, B.; Smits, J. M. M.; Gal, A. W. *Organometallics* **2003**, *22*, 3022–3024.

(18) (a) Tejel, C.; del Río, M. P.; Ciriano, M. A.; Reijerse, E. J.; Hartl, F.; Záliš, S.; Hetterscheid, D. G. H.; Tsichlis i Spithas, N.; de Bruin, B. *Chem. Eur. J.* **2009**, *15*, 11878–11889; (b) Tejel, C.; Ciriano, M. A.; del Rio, M. P.; Hetterscheid, D. G. H.; Tsichilis i Spitas, N.; Smits, J. M. M.; de Bruin, B. *Chem. Eur. J.* **2008**, *14*, 10932–10936.

(19) (a) Friedrich, A.; Drees, M.; Käss, M.; Herdtweck, E.; Schneider, S. *Inorg. Chem.* **2010**, *49*, 5482–5494; (b) Friedrich, A.; Ghosh, R.; Kolb, R.; Herdtweck, E., Schneider, S. *Organometallics*, **2009**, *28*, 708–718; (c) Meiners, J.; Friedrich, A.; Herdtweck E.; Schneider, S. *Organometallics* **2009**, *28*, 6331–6338.

(20) (a) Balaraman, E.; Gnanaprakasam, B.; Shimon, L. J. W.; Milstein, D. *J. Am. Chem. Soc.* **2010**, *132*, 16756–16758; (b) Khaskin, E.; Iron, M. A.; Shimon, L. J. W.; Zhang, J.; Milstein, D. *J. Am. Chem. Soc.* **2010**, *132*, 8542–8543; (c) Gnanaprakasam, B.; Zhang, J.; Milstein, D. *Angew. Chem. Int. Ed.* **2010**, *49,* 1468–1471; (d) Kohl, S. W.; Weiner, L.; Schwartsburd, L.; Konstantinovski, L.; Shimon, L. J. W.; Ben-David, Y.; Iron, M. A.; Milstein, D. *Science* **2009**, *324*, 74–77; (e) Gunanathan, C.; Ben-David, Y.; Milstein, D. *Science* **2007**, *317*, 790–792. (f) Kohl, S. W.; Weiner, L.; Schwartsburd, L.; Konstantinovski, L.; Shimon, L. J.W.; Ben-David, Y.; Iron, M.A.; Milstein, D. *Science* **2009**, *324*, 74. (g) Hetterscheid, D. G. H.; van der Vlugt, J. I.; de Bruin, B.; Reek, J. N. H. *Angew. Chem. Int. Ed.*, **2009**, *48*, 8178–8181.

(21) (a) de Bruin, B.; Brands, J. A.; Donners, J. J. J. M.; Donners, M. P. J.; de Gelder, R.; Smits, J. M. M.; Spek, A. L.; Gal, A. W. *Chem. Eur. J.* **1999**, *5*, 2921–2936; (b) Hetterscheid, D. G. H.; Klop, M.; Kicken, R. J. N. A. M.; Smits, J. M. M.; Reijerse, E. J.; de Bruin, B. *Chem. Eur. J.* **2007**, *13*, 3386–405.

(22) Meyer, M.; Frémont, L.; Espinosa, E.; Brandès, S.; Vollmer, G. Y.; Guillard, R. *New J. Chem.* **2005**, *29*, 1121–1124 *and references therein*.

(23) (a) Jakusch, T.; Marcão, S.; Rodrigues, L.; Pessoa, J. C.; Kiss, T. *Dalton Trans.* **2005**, 3072–3078; (b) Sóvágó, I.; Bertalan, C.; Göbl, L.; Schön, I.; Nyéky, O. *J. Inorg. Biochem.* **1994**, *55*, 67–75 *and references therein*.

(24) In non-polar solvents, like thf, solvation effects are not likely to affect cooperativity in ligand deprotonation reactions.

(25) Tejel, C.; Ciriano, M. A.; del Río, M. P.; van den Bruele, F. J.; Hetterscheid, D. G. H.; Tichilis i Spithas, N.; de Bruin, B. *J. Am. Chem. Soc.* **2008**, *130*, 5844–5845.

(26) Resonance structure **7**$^{\mathbf{A}}$ can not be fully discarded, as is clear from the only weakly increased π-back donating properties of Rh2 to the cod double bonds (as compared to Rh1).

(27) (a) Lu, C. C.; Peters, J. C. *J. Am. Chem. Soc.* **2004**, *126*, 15818–15832; (b) Owen, G. R.; Vilar, R.; White, A. J. P.; Williams, D. J. *Organometallics* **2003**, *22,* 3025–3027.

(28) Wehman-Ooyevaar, I. C. M.; Luitwieler, I. F.; Vatter, K.; Grove, D. M.; Smeets, W. J .J.; Horn, E.; Spek, A. L.; van Koten, G. *Inorg. Chim. Acta* **1996**, *252*, 55–69.

(29) Maire, P.; Sreekanth, A.; Büttner, T.; Harmer, J.; Gromov, I.; Rüegger, H.; Breher, F.; Schweiger, A.; Grützmacher, H. *Angew. Chem. Int. Ed.* **2006**, *45*, 3265–3269

(30) Hattori, T.; Matsukawa, S; Kuwata, S.; Ishii, Y., Hidai, M. *Chem. Commun.* **2003**, 510–511.

(31) (a) Cook, T. R.; Esswein, A. J.; Nocera, D. G. *J. Am. Chem. Soc.* **2007**, *129*, 10094–10095; (b) Gray, T. C.; Nocera, D. G. *Chem. Comun.* **2005**, 1540–1542.

(32) Veige, A. S.; Gray, T. G.; Nocera, D. G. *Inorg. Chem.* **2005**, *44*, 17–26.

(33) Esswein, A. J.; Veige, A. S.; Piccoli, P. M. B.; Schultz, A. J.; Nocera, D. G. *Organometallics* **2008,** *27,* 1073–1083.

(34) (a) Nocera, D. G. *Inorg. Chem.* **2009**, *48*, 10001–10017; (b) Esswein, A. J.; Nocera, D. G. *Chem. Rev.* **2007**, *107*, 4022–4047; (c) Esswein, A. J.; Beige, A. S.; Nocera, D. G. *J. Am. Chem. Soc.* **2005**, *127*, 16641–16651.

(35) Paul, N. D.; Krämer, T.; McGrady, J. E.; Goswami, S. *Chem. Commun.* **2010**, *46*, 7124–7126.

(36) Tejel, C.; Villoro, J. M.; Ciriano, M. A.; López, J. A.; Eguizábal, E.; Lahoz, F. J.; Bakhmutov, V. I.; Oro, L. A. *Organometallics* **1996**, *15*, 2967–2978.

(37) de Bruin, B.; Peters, T. P. J.; Suos, N .N. F. A.; de Gelder, R.; Smits, J. M. M.; Gal, A. W. *Inorg. Chim. Acta* **2002**, *337***,** 154–162.

(38) The single precedent of this type of reaction corresponds to the related rhodium norbornadiene complex (see reference 36).

(39) (a) Holland, P. L.; Andersen, R. A.; Bergman, R. G. *Comments Inorg. Chem.* **1999**, *21*, 115–129; (b) Caulton, K. G. *New J. Chem.* **1994**, *18*, 25–41.

(40) The differences cannot be of kinetic origin. Iridium complexes are generally kinetically slower than rhodium, or even inert in some cases, while in these reactions the iridium complex **8** reacts with bpa while the rhodium analogue **7** does not. Hence, the differences can only be explained by a reversed equilibrium distribution.

(41) Delocalization to the carbonyl moiety renders the lone pair at N2 unavailable for binding another metal. According to DFT, compound **10** is 6.7 kcal/mol more stable than its isomer with Rh coordinated to the picoline moiety and a pending carbonyl appended pyridine.

(42) (a) Dzik, W. I.; van der Vlugt, J. I.; Reek, J. N. H.; de Bruin, B. *Angew. Chem. Int. Ed.* **2011**, *50*, 3356–3358. (b) Chirik, P. I.; Wieghardt, K. *Science* **2010**, *327*, 794–795. (c) de Bruin, B.; Hetterscheid, D. G. H.; Koekoek, A. J. J.; Grützmacher, H. *Progr. Inorg. Chem.* **2007**, *55*, 247–354. (d) de Bruin, B.; Hetterscheid, D. G. H. *Eur. J. Inorg. Chem.* **2007**, *55*, 211–230; (e) Dzik, W. I.; Reek, J. N. H.; de Bruin, B. *Chem. Eur. J.* **2008**, *14*, 7594–7599; (f) Dzik, W. I.; Xu, X.; Zhang, X. P.; Reek, J. N. H.; de Bruin, B. *J. Am. Chem. Soc.*, **2010**, *132*, 10891–10902. (g) Olivos Suarez, A. I.; Jiang, H.; Zhang, X. P.; de Bruin, B. *Dalton Trans.*, **2011**, *Advance Article, DOI: 10.1039/C1DT10027K.*

(43) Perrin, D. D. W.; Armarego, L. F. *Purification of Laboratory Chemicals*, 3rd ed., Pergamon Press, Exeter, UK **1988**.

(44) Usón, R.; Oro, L. A.; Cabeza, J. A. *Inorg. Synth.* **1985**, *23*, 126–129.

(45) (a) Ahlrichs, R.; Bär, M.; Baron, H.-P.; Bauernschmitt, R.; Böcker, S.; Ehrig, M.; Eichkorn, K.; Elliott, S.; Furche, F.; Haase, F.; Häser, M.; Hättig, C.; Horn, H.; Huber, C.; Huniar, U.; Kattannek, M.; Köhn, A.; Kölmel, C.; Kollwitz, M.; May, K.; Ochsenfeld, C.; Öhm, H.; Schäfer, A.; Schneider, U.; Treutler, O.; Tsereteli, K.; Unterreiner, B.; von Arnim, M.; Weigend, F.; Weis, P.; Weiss, H. Turbomole Version 5.8, January 2002. Theoretical Chemistry Group, University of Karlsruhe; (b) Treutler, O.; Ahlrichs, R. *J. Chem. Phys.* **1995**, *102*, 346–354; (c) Turbomole basisset library, Turbomole Version 5.8, see a; (d) Schäfer, A.; Horn, H.; Ahlrichs, R. *J. Chem. Phys.* **1992**, *97*, 2571–2577; (e) Andrae, D.; Haeussermann, U.; Dolg, M.; Stoll, H.; Preuss, H. *Theor. Chim. Acta* **1990**, *77*, 123–141; (f) Schäfer, A.; Huber, C.; Ahlrichs, R. *J. Chem. Phys.* **1994**, *100*, 5829–5835; (g) Ahlrichs, R.; May, K. *Phys. Chem. Chem. Phys.* **2000**, *2*, 943–945.

(46) (a) PQS version 2.4, 2001, Parallel Quantum Solutions, Fayetteville, Arkansas, USA (the Baker optimizer is available separately from PQS upon request); (b) Baker, J. *J. Comput. Chem.* **1986**, *7*, 385–395.

(47) (a) Becke, A. D. *Phys. Rev. A* **1988**, *38*, 3098–3100; (b) Perdew, J. P. *Phys. Rev. B* **1986**, *33*, 8822–8824.

(48) (a) Lee, C.; Yang, W.; Parr, R. G. *Phys. Rev. B* **1988**, *37*, 785–789; (b) Becke, A. D. *J. Chem. Phys.* **1993**, *98*, 1372–1377; (c) Becke, A. D. *J. Chem. Phys.* **1993**, *98*, 5648–5652; (d) Calculations were performed using the Turbomole functional 'b3-lyp', which is not identical to the Gaussian 'B3LYP' functional.

(49) Schaftenaar G.; Noordik, J. H. 'Molden: a pre- and post-processing program for molecular and electronic structures', *J. Comput.-Aided Mol. Design* **2000**, *14*, 123–134.

(50) Sheldrick, G. M. SADABS, Bruker AXS, Madison, WI (USA), **1997**.

(51) Sheldrick, G. M. *SHELXL-97: Program for Crystal Structure Refinement*, University of Göttingen, Göttingen (Germany), **1997**.

(52) Farrugia, L. F. *J. Appl. Crystallogr.* **1999**, *32*, 837–838.

Graphic for Table of Contents:

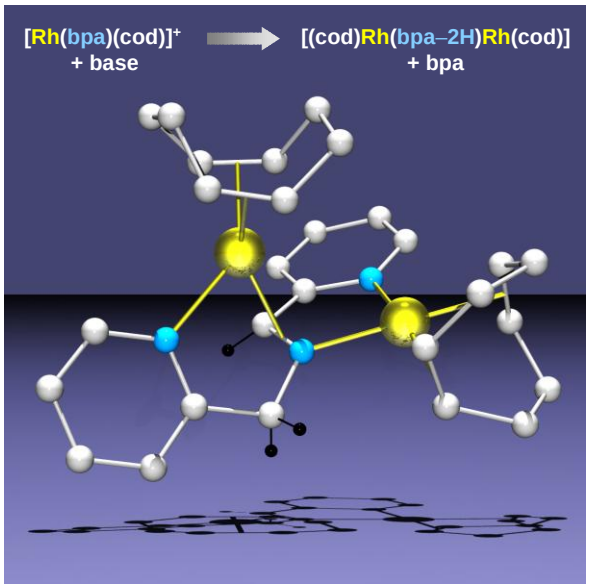

Table of Contents Synopsis:

Deprotonation of the complex $[Rh^{I}(bpa)(cod)]^{+}$ (bpa = bis(picolyl)amine) led to an unusual and spontaneous *cooperative reductive double deprotonation* producing the Rh^{-I},Rh^{I} mixed-valence complex $[(cod)Rh^{-I}(bpa–2H)Rh^{I}(cod)]$ (see Figure) with a rhodate(–I) center. The dinuclear iridium analog $[(cod)Ir^{-I}(bpa–2H)Ir^{I}(cod)]$ can be prepared, but it is unstable in the presence of 1 molar equivalent of the free bpa ligand leading to quantitative formation of the amido complex $[Ir^{I}(bpa–H)(cod)]$. The lower stability of the M^{-I} oxidation state for iridium as compared to rhodium accounts for the reported results.